AIAA JOURNAL
Vol. 33, No. 12, December 1995

In-Flight Imaging of Transverse Gas Jets Injected into Compressible Crossflows

K. C. Wang,* O. I. Smith,† and A. R. Karagozian‡
University of California, Los Angeles, Los Angeles, California 90095-1597

The development of and results from an airborne flight-test experiment to study nonreacting gas jets injected transversely into subsonic and slightly supersonic crossflows is presented. Freestream/crossflow Mach numbers in the study ranged from 0.6 to 1.2, and planar laser-induced fluorescence imaging of an iodine-seeded nitrogen jet was used to visualize the jet flow. Time-dependent images were obtained with a high-speed intensified video camera synchronized to the laser pulse rate. The entire experimental assembly was configured compactly inside a unique flight-test fixture mounted under the fuselage of NASA Dryden's F-104G research aircraft, which served as a flying wind tunnel. Recorded transverse gas jet images were then digitized to allow analysis of jet trajectory, spreading, and mixing characteristics. Comparisons of experimental results with model predictions in this transonic crossflow regime show reasonable agreement.

Nomenclature

A_j = cross-sectional area of jet nozzle at exit
A_6 = cross-sectional area of jet nozzle at transducer location; see Fig. 4
M_j = jet exit Mach number
M_∞ = freestream Mach number, upstream of jet; see Figs. 1 and 4
p_b = static pressure surrounding jet, downstream of bow shock; see Fig. 4
p_j = static pressure at jet exit
p_6 = static pressure measured at transducer location; see Fig. 4
p_∞ = freestream static pressure, upstream of jet; see Figs. 1 and 4
R = jet-to-crossflow dynamic pressure ratio or momentum flux ratio
γ_j = ratio of specific heats of jet fluid
γ_∞ = ratio of specific heats of freestream gas
ρ_j = gas density at jet exit
ρ_∞ = gas density upstream of jet; see Figs. 1 and 4

Introduction and Overview

THE transverse jet is a classical flow problem that continues to be actively studied.[1–6] Its applications include fuel injection for conventional turbojet and ramjet combustors as well as scramjet combustors, dilution jets for local cooling processes, and thrust vector control systems. In particular, a resurgence of interest in the past decade concerning scramjet technology has focused on optimizing the entrainment, mixing, and reaction processes of the injectant fuel and supersonic inlet air within the limited length of the combustor.[7–11]

A schematic diagram of the flow processes associated with the gas jet in supersonic crossflow is shown in Fig. 1. Experimental studies on transverse jets have utilized conventional mass sampling, schlieren, and shadowgraph techniques[6,12] as well as modern laser-based imaging techniques such as Rayleigh/Mie scattering and planar laser-induced fluorescence (PLIF).[4,5] Many other related experiments have been performed for incompressible flows.[13,14] Analytical and computational models have also been developed to describe the fluid dynamics of the single-phase transverse jet. Those developed at the University of California, Los Angeles, by Heister and Karagozian[1,2] and by Karagozian[15] are analytically oriented and emphasize the dynamics of the vortical structures observed to dominate the cross section of transverse jets injected into a crossflow of the same phase, whether compressible, subsonic, or supersonic. Fully numerical simulations of compressible transverse jets have also been undertaken.[8]

Some experimental data are available with which numerically predicted trajectories and mixing patterns for the compressible transverse jet can be compared, but these are limited to subsonic and higher supersonic crossflows.[4–6,12,16,17] Almost all of the supersonic crossflow data available are for freestream Mach numbers in the range $2.0 \leq M_\infty \leq 3.0$, the only exception being a few sets of data at $M_\infty = 1.4$ (Ref. 5) and 1.38 (Ref. 17). No data to our knowledge are available in the transonic crossflow regime ($0.8 < M_\infty < 1.38$).

The simple models of Heister and Karagozian[1,2] and a model update by Le[3] show reasonably good agreement with existing experimental data under both supersonic and subsonic crossflow conditions (within 15%). Yet much of the existing wind-tunnel data are for highly underexpanded jets[12]; the fact that the present and other models are most appropriate for perfectly expanded or slightly underexpanded jets presents problems with respect to model validation. Also, in some wind-tunnel experiments, the data show signs of interference by the tunnel wall on the far-field behavior of the jet.[4] In light of these issues, we are motivated to look more extensively at nearly perfectly expanded transverse gas jets in the crossflow regime where $0.8 < M_\infty < 1.4$ and to do so in such a manner that the jet is unconstrained by interaction with the opposing wall. Flight tests on an aircraft capable of flying in this flow regime (e.g., the F-104) allow us to meet these goals adequately.

In cooperation with the NASA Dryden Flight Research Center at Edwards Air Force Base, California, we utilized the F-104G research aircraft 826 as a flying wind-tunnel platform for the transverse jet experiments; a photo of the aircraft with the flight-test fixture is shown

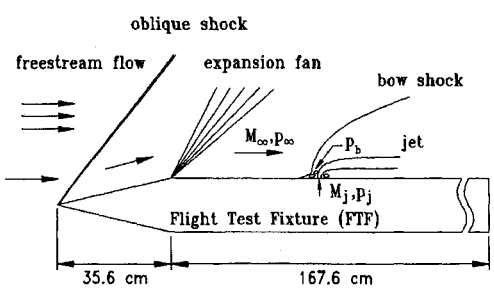

Fig. 1 Flow processes associated with gas jet in supersonic crossflow formed by flight-test fixture.

Received Nov. 1, 1994; revision received June 5, 1995; accepted for publication July 3, 1995.

*Graduate Student Researcher, Department of Mechanical, Aerospace, and Nuclear Engineering. Member AIAA.
†Professor, Department of Mechanical, Aerospace, and Nuclear Engineering.
‡Professor, Department of Mechanical, Aerospace, and Nuclear Engineering. Associate Fellow AIAA.

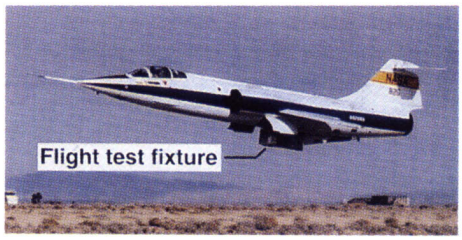

Fig. 2 Photograph of F-104G flying with flight-test fixture attached to fuselage.

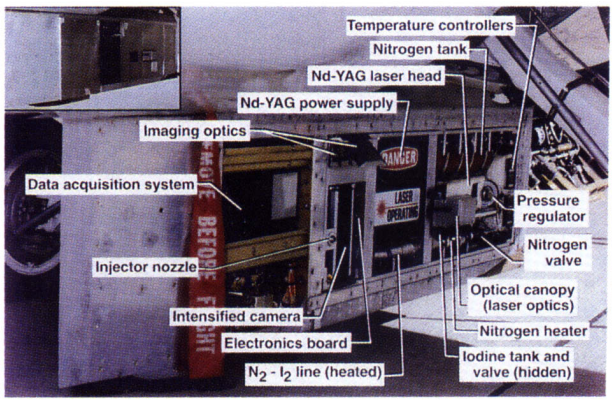

Fig. 3 Photograph of internal components of flight-test fixture; FTF with cover appears in upper left corner.

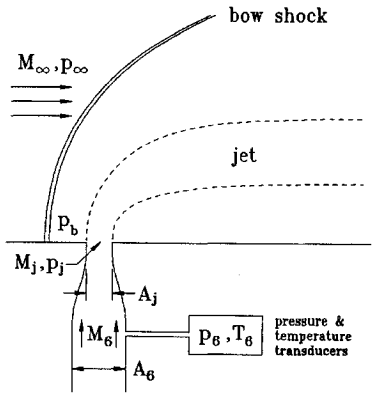

Fig. 4 Pertinent pressures and other flow properties in the vicinity of the jet nozzle exit.

in Fig. 2. During the 1960s, the Lockheed F-104G was modified to carry a low aspect ratio fin on the underside of the fuselage for the purpose of conducting panel flutter tests in a flight environment. This flight-test fixture (FTF) has evolved into a highly versatile facility for fluid mechanics research.[18] The capabilities of the FTF include 1) a large flight Mach number envelope (0.4–2.0), including the region through Mach 1.0 with no adverse effects; 2) the ability to test articles or study flowfields larger than those that can accurately be tested in wind tunnels; and 3) a larger Reynolds number and dynamic pressure envelope than most tunnels. In addition, a flight trajectory guidance system can uplink engineering parameters calculated on a ground-based computer (using aircraft and/or FTF telemetry) to the cockpit display so that the pilot can maintain desired flight-test conditions. Given its many capabilities and advantages, the F-104/FTF testbed suits the present experimental needs quite well.

Description of Experiment

PLIF Imaging

As illustrated in Fig. 1, in the present experiment the gas jet was injected normally into the crossflow from the side of the FTF, turning immediately into the freestream. Iodine-seeded nitrogen was used as the injectant since previous work has suggested that jet penetration and spreading are insensitive to injectant molecular weight[19]; hence, the injectant here could represent air or fuel.

The trajectory and spreading of the jet here were determined by illuminating a streamwise planar cross-section of the nitrogen jet with a sheet of laser light. PLIF of the iodine seed allowed jet images to be visualized. The second harmonic of a Nd:YAG laser at 532.25 nm was used to pump several lines in the R and P branches of the $B \leftarrow X$ transition for I_2: the R(56)(32-0) line at 18788.348 cm^{-1}, the P(83)(33-0) and R(134)(36-0) lines around 18787.814 cm^{-1}, and the P(53)(32-0), P(103)(34-0), and P(159)(39-0) lines around 18788.453 cm^{-1} (Ref. 20). A Q-switched (pulsed) diode pumped Nd:YAG laser (Adlas DPY 321 QD) as used, operating in the broadband mode with visible green/yellow light. Operating in this mode, the laser linewidth was approximately one wave number, so that none of the lines listed were individually resolved; rather, all of the lines were simultaneously excited.

Flowfield images were captured by a high-speed gated intensified video camera synchronized to the laser pulse rate and equipped with appropriate optical filters to improve the signal-to-noise ratio. An ITT image intensified solid-state charge-coupled device (CCD) camera (F4577) was used, incorporating a Generation II image intensifier, an 11-mm CCD sensor, and integrated electronics to produce a very high-resolution RS-170 video signal. The image intensifier used a microchannel plate (MCP) current amplifier with an S20

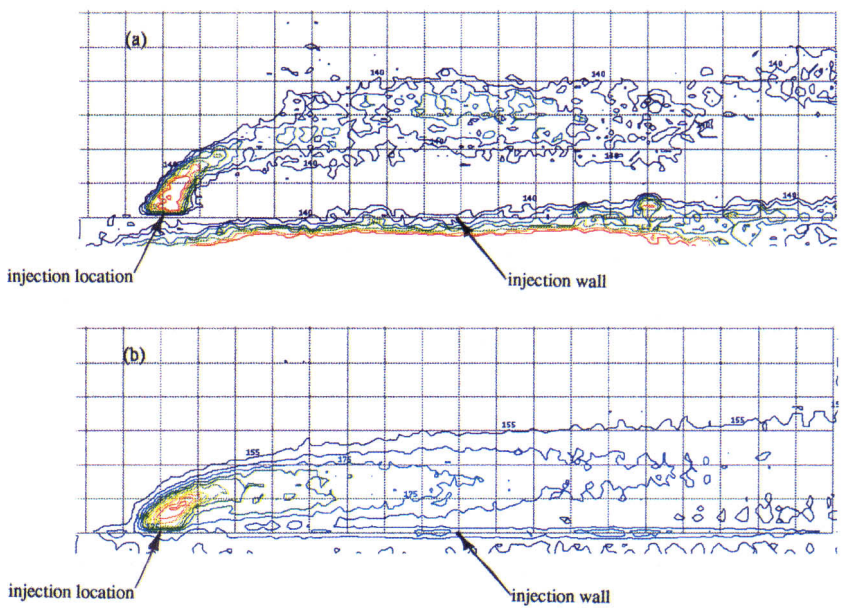

Fig. 5 Iodine concentration contours, where high concentrations of iodine appear in red and yellow, lower concentrations appear in green and blue; each grid marking shown represents one jet diameter D; for a) subsonic crossflow conditions corresponding to experimental case a and b) supersonic crossflow conditions corresponding to experimental case g (cf. Table 1).

photocathode. The CCD was a Texas Instruments TC241 488(V) × 754(H) pixel, frame-transfer device with a 6.6 × 8.8 mm image format. The electronics provide photocathode gating, gain control, and an automatic iris control signal. The F4577 uses a tapered fiber optic coupling between the intensifier and CCD to achieve high-efficiency image transfer. Background light was rejected using an Oriel high-pass interference filter with a 530 nm cut-on.

Jet Characteristics

Transverse jet behavior has been found to be strongly correlated with the jet-to-freestream momentum flux ratio.[4,14,21] For an ideal gas, the momentum flux ratio is equivalent to the jet-to-freestream dynamic pressure ratio and is expressed as

$$R = \frac{\gamma_j p_j M_j^2}{\gamma_\infty p_\infty M_\infty^2} = \frac{\rho_j U_j^2}{\rho_\infty U_\infty^2}$$

where the subscript j corresponds to jet exit conditions and ∞ corresponds to freestream conditions ahead of a bow shock, if present. The ratios of specific heats for the jet and the crossflow were approximately the same in the present experiments. The jet Mach number was fixed near $M_j = 1$ since modeling of the gas jet in a supersonic crossflow indicates that jet penetration can be maximized when the injection Mach number is slightly greater than one.[1] The freestream Mach number in these experiments was varied from approximately $M_\infty = 0.6$–1.2.

Flight-Test Fixture and Experimental Procedure

The experimental apparatus was comprised of three subsystems: one containing the laser and its associated optics, one containing the intensified camera and its filters and mirrors responsible for imaging the fluorescent jet, and a jet formation subsystem that included all components involved in the storage, pressure regulation, heating, and flow control of the nitrogen gas and iodine seed. A photograph of the flight test fixture appears in Fig. 3. The following summarizes the features of these subsystems; specific details may be found in Ref. 22.

The laser sheet was formed in flight by means of a −6.35-mm focal length front surface cylindrical mirror that expanded the beam perpendicularly to the FTF in the streamwise direction. A high-reflectivity mirror housed in the optical canopy acted as a turning mirror, positioning the light sheet on the plane of the jet. This positioning was dependent on the aircraft's angle of attack (approximately +3 deg alpha for the F-104G in level flight); provision for adjustment was made via a multiaxis kinematic mirror mount. A 300-mm focal length cylindrical lens at the front of the canopy acted to thin the sheet.

Iodine flourescence in the jet was imaged onto the intensifier focal plane using a system of one internal and one external mirror, along with a standard Nikon 28-mm f2.8 camera lens on the F4577. The internal mirror was oriented at a 45-deg angle and mounted just above the camera lens, allowing an outward view. This arrangement resulted in a viewable area of about 11.5 × 16.6 cm in the plane of the jet. The framing rate of the camera was 30 Hz.

Nitrogen for jet formation was stored at pressures up to 3000 psig in a 5.1-liter high-pressure cylinder. The jet was only operated when the experiment reached a desired flight-test condition, at which time a solenoid valve was activated for a preprogrammed duration (variable from 6 to 13 s). This time period allowed for virtually steady-state jet behavior to be achieved, as verified later from PLIF images. Iodine vapor was seeded into the main nitrogen flow at a tee-branch in concentrations of at least 2000 ppm; seeding rates were regulated by controlling the temperature and, thus, the pressure of the iodine reservoir/cell. Uncertainties in iodine concentrations are of the order 200 ppm. After seeding, the N_2–I_2 mixture was carried in heated stainless-steel lines and, finally, passed through an aluminum nozzle to produce a sonic jet at the nozzle exit/throat. The nozzle exit was machined to a diameter of 7.2 mm.

Upon reaching a desired test condition, the pilot fired the experiment, then stabilized the flight Mach number, altitude, and angle of attack as best as possible for the duration of the experiment. The entire experiment was operated solely by the pilot in flight. Images of the illuminated jet were viewed in real time during the flights as well as recorded on VHS and beta tape formats for postflight review.

Results

Four individual flight tests (takeoffs and landings) were successfully performed at NASA Dryden in January of 1994. Two of the flights, numbered 1410 and 1411, were for gas jets injected into uniform crossflow, the cases under examination here. The other two flights, 1412 and 1415, contain test data for a jet injected downstream of a rearward-facing step, a case reported in a separate paper.[23] For most flights, several supersonic crossflow test points and several subsonic points were achieved. The various jet and flight conditions run for these experiments are summarized in Table 1.

From flight-test data, jet conditions were evaluated as follows, with reference to the nozzle schematic shown in Fig. 4. The pressures p_b (surrounding the jet, behind a bow shock, if present) and p_6 (at a pressure transducer upstream of the converging section) were measured in flight. The nozzle exit was situated at a local area minimum, and isentropic flow was assumed in the nozzle. The upstream Mach number M_∞ was measured using a pitot probe situated in the noseboom of the F-104G (see Fig. 1), in addition to incorporating prior flight-test data[18] to account for downwash, body, and shock wave effects.

Clearly, if $p_b/p_6 \leq 0.528$, the nozzle can be considered to be choked; $M_j = 1$ and p_j may be evaluated from the area ratio A_6/A_j and p_6. If the pressure ratio $p_b/p_6 > 0.528$, however, then the nozzle is likely not to be choked ($M_j < 1$), but it is likely that $p_j = p_b$ for subsonic exhaust. For this case, M_j can be evaluated from the area ratio $A_6/A_j = 2$ and from $p_b/p_6 = p_j/p_6$, again assuming isentropic flow. Errors do arise in p_j due to data/measurement scatter (6–12%), yielding error bounds believed to be of the order 7–13% in the estimate for R and of the order 1% in M_j. Errors in crossflow conditions are of the order 2% for M_∞.

Iodine PLIF images for the jet in crossflow were obtained for the duration of all flights shown in Table 1. Iodine concentration contours were produced by averaging iodine PLIF images over approximately 135 frames, representing the latter 75% of the duration of jet injection, and then analyzing the images. The nozzle temperature varied over the initial 25% of the jet injection period; hence, these images were not included in the averaging. The latter 75% of the jet injection period produced very stable transverse jets.

Typical iodine contours for subsonic and supersonic crossflow conditions are shown in Figs. 5a and 5b. Highest concentrations of iodine are apparent in the near-field potential core region of the jet that disappears within a few jet diameters downstream of injection. Contours appearing below the injection wall result from scattered light off the wall and should be ignored. The spread of the jet downstream is evident through the spatial growth of the regions of lower iodine concentrations. As would be expected, the degree of jet turning is increased with higher crossflow Mach number.

From images such as those in Figs. 5a and 5b it is possible to determine the locations of maxima in iodine concentration. This determination follows a given contour and evaluates the locus at which the slope of the contour becomes zero. The loci of concentration maxima roughly correspond to the trajectory of the vortex pair associated with the jet cross section, since most of the jet fluid becomes concentrated within a few diameters into the vortical structures.[13,14] It should be noted that these maxima in iodine concentrations do not correspond exactly to the loci of velocity maxima, however, but somewhat lag this actual jet centerline, as does the vortex pair trajectory.[14]

Table 1 Jet and freestream conditions for different cases flown

Case	M_∞	M_j	p_j/p_∞	R	Flight no.
a	0.614	1.0	1.037	2.75	1410-1
b	0.713	0.982	1.00	1.90	1411-2
c	0.730	1.0	1.095	2.055	1410-2
d	0.808	0.970	1.00	1.445	1411-1
e	0.823	1.0	1.082	1.598	1410-8
f	0.918	0.996	1.04	1.23	1410-7
g	0.975	0.955	1.09	1.04	1410-6
h	0.978	0.851	1.10	0.833	1411-4a
i	1.123	0.77	1.13	0.528	1411-5
j	1.21	1.0	1.21	0.823	1410-5

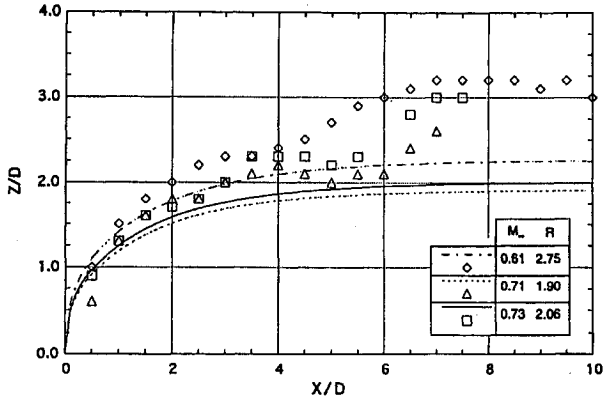

Fig. 6a Comparisons of experimentally determined loci of iodine concentration maxima with vortex pair trajectories predicted by the models in Refs. 1–3; test conditions correspond to conditions, a, b, and c given in Table 1.

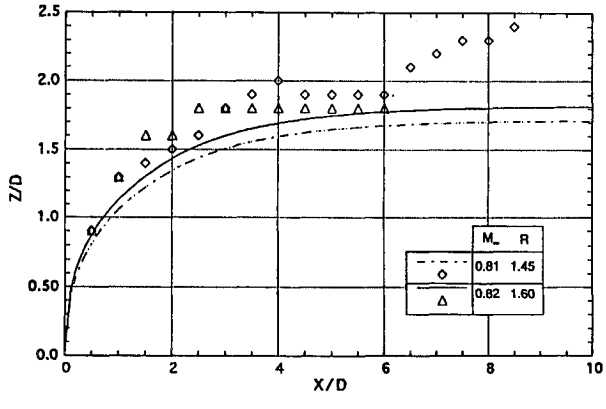

Fig. 6b Comparisons of experimentally determined loci of iodine concentration maxima with vortex pair trajectories predicted by the models in Refs. 1–3; test conditions correspond to conditions d and e given in Table 1.

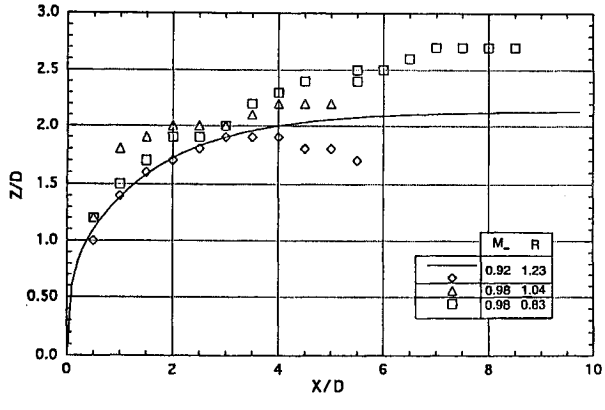

Fig. 6c Comparisons of experimentally determined loci of iodine concentration maxima with vortex pair trajectories predicted by the models in Refs. 1–3; test conditions correspond to conditions f, g, and h given in Table 1.

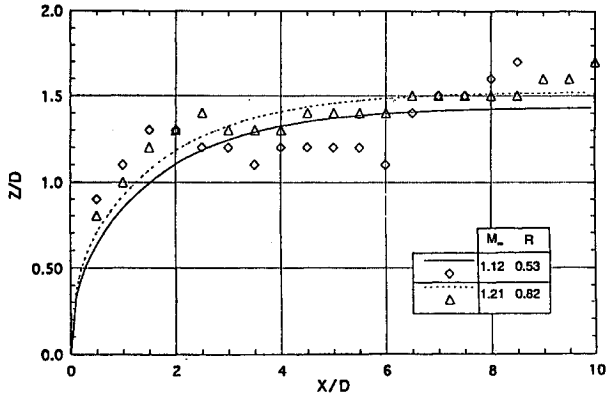

Fig. 6d Comparisons of experimentally determined loci of iodine concentration maxima with vortex pair trajectories predicted by the models in Refs. 1–3; test conditions correspond to conditions i and j given in Table 1.

Measured loci of concentration maxima thus may be compared with vortex pair trajectories predicted for compressible transverse jets by earlier models.[1–3] These comparisons are shown in Figs. 6a–6d, where experimental data are shown by the symbols and where the mass balance modification described in Le[3] and Karagozian et al.[23] was used for the model results. Figures 6a and 6b describe measured and calculated concentration maxima for gas jets injected into subsonic crossflow (cf. Table 1). Here we see a reasonable correspondence between the model and experimental data. It should be noted that the similarities in test conditions between cases b and c (Fig. 6a) and between cases d and e (Fig. 6b) provide a rough measure of the repeatability of the experiments from flight to flight. It should also be noted that for all of the subsonic crossflow comparisons shown the jet-to-crossflow momentum flux ratio R exceeds unity. Under these circumstances, earlier experiments[4,14] indicate that the jet momentum is probably high enough for a vortex pair to form and be dominant in the jet far field; hence, the model is appropriate for these cases.

The subsonic crossflow cases very near Mach one, cases f–h, are shown in Fig. 6c. The model predictions for case f ($M_\infty = 0.92$, $R = 1.23$) correspond reasonably well to experimental measurements of trajectory. For cases g ($M_\infty = 0.98$, $R = 1.04$) and h ($M_\infty = 0.98$, $R = 0.83$), one finds an interesting trend in the experimental data. There actually appears to be an increase in experimental jet penetration for these cases over the slightly lower crossflow Mach number cases (e.g., as shown in Fig. 6b), despite the fact that the momentum flux ratio R is substantially lower in cases g and h than in cases e ($M_\infty = 0.82$, $R = 1.60$) and f. This observation contradicts conventional wisdom that says that jet penetration increases with increasing momentum flux ratio R (Refs. 4, 6, 14, and 21). The model trends follow the conventional wisdom, i.e., that a lower degree of jet penetration occurs with lower momentum flux ratios R. In fact, the model solution does not even converge for the experimental conditions in cases g and h; this may be due to the fact that strong nonlinearities arise close to Mach one that are not adequately represented in the model. The fact that experimental cases g and h exhibit similar behavior to each other at similar M_∞ values, yet represent two different flights (1410 and 1411), suggests that this unusual behavior may not result from experimental error. The behavior is likely to be an outcome of the near-sonic crossflow Mach number condition and bears further investigation.

Figure 6d describes results and model comparisons for slightly supersonic crossflow conditions. In case i ($M_\infty = 1.12$, $R = 0.53$), the momentum flux ratio R is well below unity, raising questions about the nature of the transverse jet. Such a low-momentum flux ratio may preclude the actual existence of a vortex pair in the flowfield and, hence, the appropriateness of comparison with a vortex model. Interestingly, though, the model does appear to correspond well to experimental data shown in Fig. 6d; note that the penetration is substantially lower in these slightly supersonic cases than in the slightly subsonic cases shown in Fig. 6c.

It is also interesting to note that in both subsonic and supersonic crossflow cases the jets often experience a rather sudden increase in penetration near six jet diameters downstream of injection. Prior wind-tunnel studies[4,14,17] also indicate slight increases in penetration downstream of the injection point; this previously had been thought to be associated with the influence of the opposite wall of the tunnel, perhaps resulting from the reflection of oblique waves. The present studies show that this rather abrupt increase in penetration is not due to opposite wall effects but, rather, is likely to arise from an alteration in fundamental jet structure, perhaps coincident with an alteration in the strength of the vortices that dominate the jet cross section.

Cases with higher crossflow Mach numbers (1.4–1.8) and low momentum flux ratios R (of the order 0.7) were also flown in this series of experiments, although the degree of jet penetration for these cases is extremely low, again possibly indicative of the absence of vortical structures altogether.

Conclusions

We have presented the development of and results for a unique flight-test experiment to study nonreacting gas jets injected normally into subsonic and slightly supersonic crossflows. Comparison of experimental jet penetration with vortex model predictions shows reasonably good agreement, validating the model in a regime previously not explored experimentally.

Many of the fundamental features of transverse jets in compressible crossflows were observed in the present experiments, even though the present studies, unlike wind-tunnel tests, were devoid of opposite wall effects. Very close to sonic crossflow conditions, however, the dependence of trajectory on momentum flux ratio appears to contradict conventional transverse jet behavior.

In performing these gas jet experiments, we have also successfully applied traditionally ground-based laser diagnostics and imaging techniques to fully realistic in-flight environments, suggesting the potential for future interrogations of realistic, fundamental compressible flows in flight.

Acknowledgments

This work is supported by the NASA Dryden Flight Research Center under Grant NCC-2-374. The authors wish to acknowledge the invaluable assistance of NASA technical monitors Albion H. Bowers and Kenneth W. Iliff, assistance in plotting by B. J. Petersen, and helpful discussions with Jim McDaniel of the University of Virginia and Dimitri Papamoschou of the University of California, Irvine.

References

[1]Heister, S. D., and Karagozian, A. R., "Gaseous Jet in Supersonic Crossflow," *AIAA Journal*, Vol. 28, No. 5, 1990, pp. 819–827.

[2]Heister, S. D., and Karagozian, A. R., "Vortex Modeling of Gaseous Jets in a Compressible Crossflow," *Journal of Propulsion and Power*, Vol. 6, No. 1, 1990, pp. 85–92.

[3]Le, A. T., "Transverse Gaseous Jet Injection Behind a Rearward-Facing Step into a Supersonic Crossflow," M.S. Thesis, Dept. of Mechanical, Aerospace, and Nuclear Engineering, Univ. of California, Los Angeles, CA, June 1991.

[4]McDaniel, J. C., and Graves, J., "Laser-Induced Fluorescence Visualization of Transverse Gaseous Injection into a Nonreacting Supersonic Combustor," *Journal of Propulsion and Power*, Vol. 4, No. 6, 1988, pp. 591–597.

[5]Lee, M. P., McMillan, B. K., Palmer, J. L., and Hanson, R. K., "Planar Fluorescence Imaging of a Transverse Jet in a Supersonic Crossflow," *Journal of Propulsion and Power*, Vol. 8, No. 4, 1992, pp. 729–735.

[6]Papamoschou, D., and Hubbard, D. G., "Visual Observations of Supersonic Jets," *Experiments in Fluids*, Vol. 14, 1993, pp. 468–476.

[7]Northam, G. B., and Anderson, G. Y., "Survey of Supersonic Combustion Research at Langley," AIAA Paper 86-0159, Jan. 1986.

[8]Uenishi, K., and Rogers, R. C., "Three Dimensional Computation of Mixing of Transverse Injector in a Ducted Supersonic Airstream," AIAA Paper 86-1423, June 1986.

[9]Schetz, J. A., and Billig, F. S., "Studies of Scramjet Flowfields," AIAA Paper 87-2161, June 1987.

[10]Kumar, A., Bushnell, D. M., and Hussami, M. Y., "A Mixing Augmentation Technique for Hypervelocity Scramjets," AIAA Paper 87-1882, 1987.

[11]Chitsomboon, T., Northam, G. B., Rogers, R. C., and Diskin, G. S., "CFD Prediction of the Reacting Flowfield Inside a Subscale Scramjet Combustor," AIAA Paper 88-3259, July 1988.

[12]Zukoski, E. E., and Spaid, F. W., "Secondary Injection of Gases into a Supersonic Flow," *AIAA Journal*, Vol. 2, No. 10, 1964, pp. 1689–1696.

[13]Broadwell, J. E., and Breidenthal, R. E., "Structure of Mixing of a Transverse Jet in a Cross Flow," *Journal of Fluid Mechanics*, Vol. 148, 1984, pp. 405–412.

[14]Kamotani, Y., and Greber, I., "Experiments on a Turbulent Jet in Cross Flow," *AIAA Journal*, Vol. 10, No. 11, 1972, pp. 1425–1429.

[15]Karagozian, A. R., "An Analytical Model for the Vorticity Associated with a Transverse Jet," *AIAA Journal*, Vol. 24, No. 3, 1986, pp. 429–436.

[16]Manela, J., and Seginer, A., "Jet Penetration Height in Transonic Flow," *AIAA Journal*, Vol. 24, No. 1, 1986, pp. 67–73.

[17]Orth, R. C., Schetz, J. A., and Billig, F. S., "The Interaction and Penetration of Gaseous Jets in Supersonic Flow," NASA CR-1386, July 1969.

[18]Meyer, R. R., "A Unique Flight Test Facility: Description and Results," 13th International Council of the Aeronautical Sciences Congress/AIAA Aircraft Systems and Technology Conf., ICAS Paper 82-5.3.3, Aug. 1982.

[19]Torrence, M. G., "Effect of Injectant Molecular Weight on Mixing of a Normal Jet in a Mach 4 Airstream," NASA TN D-6061, Jan. 1971.

[20]Simmons, J. D., and Hougen, J. T., "Atlas of the I_2 Spectrum from 19,000 to 18,000 cm^{-1}," *Journal of Research of the National Bureau of Standards, Section A: Physics and Chemistry*, Vol. 81A, 1977, p. 25.

[21]Holdeman, J. D., and Walker, R. E., "An Empirical Model for the Mixing of a Row of Dilution Jets with a Confined Crossflow," NASA TM X-71787, 1976.

[22]Wang, K. C., "In-Flight Imaging of Transverse Gas Jets Injected into Transonic and Supersonic Crossflows," M.S. Project, Univ. of California, Los Angeles, CA, 1993; also NASA CR-186031, Nov. 1994.

[23]Karagozian, A. R., Wang, K. C., Le, A.-T., and Smith, O. I., "Modeling and In-Flight Imaging of Transverse Gas Jets Injected Behind a Rearward-Facing Step," AIAA Paper 96-0914, Jan. 1996.